Journal of Catalysis 306 (2013) 30–37

Contents lists available at SciVerse ScienceDirect

Journal of Catalysis

journal homepage: www.elsevier.com/locate/jcat

Fatty acid methyl esters into nitriles: Acid–base properties for enhanced catalysts ☆

A. Mekki-Berrada [a], S. Bennici [a], J.P. Gillet [b], J.L. Couturier [b], J.L. Dubois [c], A. Auroux [a,*]

[a] IRCELYON, UMR5256 CNRS – Université Lyon1, 2 Avenue A. Einstein, 69626 Villeurbanne Cedex, France
[b] ARKEMA, Centre de Recherche Rhône Alpes, Pierre Bénite, 69493 Cedex, France
[c] ARKEMA, Direction Recherche & Développement, 420 Rue d'Estienne d'Orves, 92705 Colombes, France

ARTICLE INFO

Article history:
Received 27 March 2013
Revised 24 May 2013
Accepted 29 May 2013
Available online 3 July 2013

Keywords:
Fatty nitrile
Biomass
Microcalorimetry
Acid–base catalysis

ABSTRACT

Fatty nitriles have lately become of interest in the frame of biofuels or for the valorization of the oil part of biomass as fine chemicals such as polymers. The production of long-chain fatty nitriles by direct reaction of esters with ammonia has however not been academically extensively studied, although several catalysts were developed and published in patents. Acid–base features are implicitly considered as leading the catalysis of this reaction, but no direct correlation was investigated with any nature or number of acidic or basic sites. The present study aims at understanding which sites are responsible of this reaction and thus how to design better catalysts. Strong acidity correlates at 300 °C for ester conversion and nitrile yield, suggesting a common nature of the reaction among all kinds of catalysts. An upper strength limit, over which undesirable side-products appear, was evaluated, and the factors influencing the production of N-methyl amide were analyzed.

1. Introduction

Nitriles are platform molecules that are useful in medicine as well as in polymer chemistry. Besides, in the frame of renewable energy resources, the valorization of non-edible biomass into biofuels and fine chemicals has become a major field of research, and the conversion of the oil part of biomass, that is, triglycerides, into fatty esters and nitriles has been envisaged for biofuel production [1,2]. Nitriles have a high energy density which makes them attractive to be investigated as aviation fuels, even though the possibility of NOx exhaust has to be cared about. Their use as fine chemicals however brings the necessity of controlling the chain's nature, especially regarding the unsaturations. Indeed, the nature of commonly used catalysts and also, and perhaps mainly, the high working temperature of the nitrilation processes are the source of isomerization and several side-reactions, such as Piria, Diels–Alder, or peroxidation in α position of the unsaturations (Fig. 1). Thus, in order to produce higher added value nitriles with control over the fatty chain, we can aim at reducing the operating temperature or the contact time with the catalyst, which can be achieved in a gas-phase reactor.

The nitrilation of fatty acids or esters by direct reaction with ammonia is mainly performed via two processes: first the batch one, where the acid reactant is in liquid phase and the nitrile remains in the reactor; second the gas-phase continuous one, where the acid is vaporized prior to a catalytic bed, through which it is passing together with ammonia. While the gas-phase process (few seconds contact time) consumes energy for the vaporization of the reactant and then could lead to modification of the carbon chain in the evaporation chamber before the catalytic bed, the batch liquid-phase process needs few hours of reaction at high temperature, where side-reactions are likely to happen, especially with unsaturated chains. Thus, the gas-phase process is usually more adapted to short carbon chains ($C \leqslant 12$) and to unsaturated carbon chains, since the contact time with the catalyst is short, whereas the liquid-phase process is more adapted to long carbon chains ($C \geqslant 12$) and especially saturated chains. A previous study focused on the liquid-phase batch process [3], and the scope of the present study is the transformation of shorter chain fatty esters (C12:0) in a gas-phase continuous process in the attempt of decreasing the working temperature lower than the state-of-the-art. Investigations on mono-unsaturated material are under progress and will not be addressed in the present article.

Catalyzed direct reaction of acids with ammonia in gas phase for the production of nitrile was first reported in 1916 by Van Epps and Reid [4], using alumina and thoria and operating at 500 °C for a 85% yield in acetonitrile, while no reaction was occurring when starting from the ethyl ester. However, in 1918, Mailhe [5] performed the conversion of ethyl acetate into acetonitrile with the

* Corresponding author.
E-mail address: aline.auroux@ircelyon.univ-lyon1.fr (A. Auroux).

0021-9517/$ - see front matter © 2013 The Authors. Published by Elsevier Inc. All rights reserved.
http://dx.doi.org/10.1016/j.jcat.2013.05.032

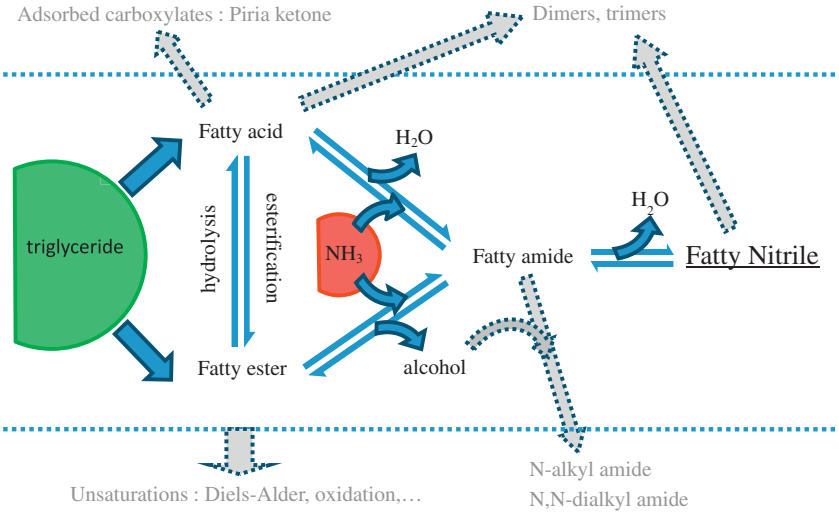

Fig. 1. Reaction scheme of the conversion of fatty esters into nitriles by direct reaction with ammonia, with the possible side-reaction.

same catalysts and same temperature. Then in 1931, Mitchell and Reid [6] performed a more extensive study with silica gel at 400–575 °C (optimum at 500 °C) on a large variety of acids and esters. The catalyst was stable for reactions with acids, whereas with esters it was rapidly fouled, probably due to the formation of aldehyde from the produced alcohol. Besides, such as described by Ralston et al. in 1935–1936 [7], some "cracking" is occurring above 400 °C on the long-chain acids and esters. Ralston et al. present high-temperature pyrolysis on alumina bed at 400–600 °C as a way of producing shorter nitriles and hydrocarbons out of long-chain compounds, preventing the formation of heavy side-products such as polymers or resins; however, further stages of separation and purification are then needed. Afterward, most advances are recorded in the patent literature, such as Wortz in 1940 [8], reporting the preparation of long-chain ($C \geqslant 8$) aliphatic nitriles from acids of the same chain length and at 425–450 °C, in contradiction with Ralston's earlier statements. Several metal oxide dehydrating catalysts are presented and the ratio of ammonia to acid is of 2.5. Above 450 °C, cracking is reported, while below 425 °C, severe decrease in conversion is observed. Then in 1992, Akikubo and Takaoka [9] reported the conversion at lower temperature, that is, "200–400 °C," of fatty acids or esters of carbon chain length from 6 to 22. Conversion of methyl laurate at 1–3 g/h, performed at 300 °C on several catalysts (mean residence time of 4–13 s), is given as an example, displaying good results for oxides of Zr, Ta, Ga, In, Sc, Nb, Hf, Fe, Zn and Sn, and bad results with oxides of Si, Mn, V and W; no results were disclosed at significantly lower temperature. However, high acid strength is pointed out as a source of side-reactions, and oxides of zirconium or potassium, as well as alkali impregnated alumina, appeared to display less of these drawbacks. The main problem with starting from an ester is the handling of the produced alcohol, not only because it may foul the catalyst, but also because it induces side-products. Takaoka et al. reported in 1998 [10] a series of zirconia-based catalysts in order to reduce the amount of such side-products, especially N-methyl-amide. Multivalent metal cations (Al, Sb, Zn, Ce, V, Nb, Ta, Cr, Mn, Fe, Co, Ni, and lanthanides) showing no strong acidity were impregnated at around 0.4 wt% on zirconia, performing a 96% conversion of methyl laurate at 1 g/h at 300 °C, displaying low amounts of N-methyl-amide in the heavy fraction and of methylamine in the lighter fraction (water, methanol, ammonia). Lately, solutions to overcome the question of methylated side-products follow the pathway of ammoxidation of alcohols, recently performed at "240–290 °C" using both dehydrating and dehydrogenating catalysts mixed in a catalytic bed [11], and lauryl alcohol conversion is presented to reach 98% at 300 °C, with a 94% yield of lauronitrile for about 4 g/h of reactant. Recent academic literature is quite scarcer concerning these issues; however, Bizhanov et al. [12] reported in 1985 a kinetic study of the nitrilation at 300 °C of mixtures of aliphatic acids of 10–22 carbon chain length. By using alumina catalyst, they obtained almost full conversion at 40 min contact time and observed zero order kinetics for the formation of amide and nitrile with 123.3 mmol s^{-1} and 97.7 mmol s^{-1}, respectively. Although the choice of esters as starting reactants can be the source of fouling or pollution of the product, their comparatively higher vapor pressure is of high interest (about twice larger at 250 °C). Furthermore, some biomass sources are more easily transformed into esters than into acids; thus, the overall conversion of triglycerides into fatty nitriles can become more interesting via esters.

2. Experimental

Commercial zinc oxide (Sigma–Aldrich), γ-alumina (DEGUSSA), niobium oxide (STARCK), zirconia (Norpro St-Gobain), zeolite H-MFI Si/Al 28 (Sud Chemie AG), faujasite HY with a 5.1:1 mol ratio of SiO_2/Al_2O_3 (Alfa Aesar), tungsten oxide (Fluka), bentonite (KSF/O Sud Chemie), titanium dioxide (Degussa P25), phosphotungstic acid on TiO_2, phosphated zirconia (Norpro St-Gobain), H_3PO_4/SiO_2 (Johnson Matthey), silica–alumina Siralox 30 and Siralox 40-450 (SASOL), hydrotalcites (Mg/Al = 3 [13] and Norpro St-Gobain), hydroxyapatites (Fluidinova 1.66 reference nanoXIM.HAp402 [14] and Ca/P = 1.66 calcined at 400 °C following Lamonier et al. procedure [15]), magnesium oxide (MERCK), $Cs_{3.0}PW_{12}O_{40}$ (from Lefebvre et al. [16]) and $Cs_{2.5}H_{1.5}SiW_{12}O_{40}$ (Nippon-Kokan Kabushiki Kaisha), boron oxide (STREM), iron (III) oxide hydrated (Aldrich), aluminum fluoride 55% (from Brunet et al. [17]) were used. Zinc–indium mixed oxides and γ-alumina were prepared and characterized in a previous article [18]. Tungstated zirconia "16%WO_x/ZrO_2" was prepared by calcination of commercial tungstated zirconium hydroxide (MEL Chemicals) and "24%WO_x/ZrO_2" as well as every M/ZrO_2 (M = Al, Fe, Co, Zn, each at 0.4 wt%) was prepared by incipient wetness impregnation [19]. Boron-containing alumina's preparation was performed by Dubois and Fujieda [20].

Lauric acid methyl ester (98+%, Sigma–Aldrich) was used as reactant in this study. Reference material for GC–FID and GC–MS was dodecanenitrile (99%, Sigma–Aldrich), dodecanamide (>98%, TCI), and dodecanoic acid (98%, Alfa Aesar).

The specific surface area (BET: Brunauer–Emmet–Teller) was determined by nitrogen adsorption at 77 K on an ASAP 2020

(Micromeritics). Adsorption microcalorimetry coupled with volumetry was used in order to evaluate the acid–base features of catalysts in matters of amount and strength [21]. After pretreatment of the catalyst at 300 °C under vacuum overnight, the calorimetric cell is inserted inside a C80 microcalorimeter from Setaram, set at 80 °C, while accurate dosing of adsorption of NH_3 or SO_2 is performed. Cycles of adsorption–desorption–readsorption provide measurement of the irreversible volume of adsorption by difference of the adsorbed and readsorbed volumes at 27 Pa equilibrium pressure, this is an estimation of the number of chemisorption sites ($\mu mol\ m^{-2}$), while the successive thermograms (integrated amount in J) and corresponding adsorbed quantities (in $\mu mol\ g^{-1}$) provide measurement of the strength of adsorption sites ($kJ\ mol^{-1}$). Adsorption of ammonia probes the acidic sites, while adsorption of sulfur dioxide probes the basic sites. The number of strong acid sites corresponds to adsorption energies of ammonia higher than 120 $kJ\ mol^{-1}$.

The experiments have been carried out on a lab-scale gas-phase continuous process consisting of a vertical downstream stainless steel microreactor provided by controlled flow rates of reactants and connected downstream with a series of condensers in order to collect heavy products together on one side and methanol, water, ammoniated water, methylamine, dimethyl-ether if any on the other side. The microreactor consists of two connected capacities: upstream side is the evaporation chamber where liquid ester is dipped inside the heated volume and blown downwards by a controlled nitrogen flow (Brooks mass flow meter, range 3–30 $ml\ min^{-1}$) and downstream is the catalytic bed of 1.60 ml volume on a stainless steel frit disc (Interchrom, pore size 2 μm). The evaporation chamber and the catalytic bed are separated by a stainless steel grid, enhancing the evaporation surface for the possibly remaining liquid ester. Ammonia flow is controlled (Brooks mass flow meter, range 4–40 $ml\ min^{-1}$) and delivered directly at the top of the catalytic bed, via a vertical tube through the evaporation chamber, ensuring that first contact between both reactants happens in the catalytic bed or at its surface, and preventing possible amide condensation above the bed. The microreactor is disposed inside a vertical furnace, ensuring a control over the catalytic bed's temperature (stability within 1 °C at 300 °C) and on the evaporation chamber's performance. Contrary to examples of the patent literature which evaporate the ester beforehand, liquid ester is here delivered to the evaporation chamber and controlled by a peristaltic pump (Gilson Minipuls 3), and the heating provided to the evaporation chamber (>2.5 W) and the flow parameters ensure full evaporation of the ester (<1 W in the present tests). The tubing for the peristaltic pump (0.50 mm inner diameter) was chosen in order to provide 0.5–5 $g\ h^{-1}$ of methyl laurate and calibrated on the peristaltic pump. The contact time is defined here as the ratio of the catalytic bed's volume (ml) by the combined flow rates ($ml\ s^{-1}$). Moreover, the mass and composition of the outflowing heavy gases were monitored in order to ensure the mass balance of the setup. The product stream is brought to a first condenser thermostated at 150 °C, condensing heavy products such as ester, acid, amide or nitrile in a graduated vat, and then, the remaining flow is brought to a second condenser thermostated by industrial water at 12–15 °C and to a dry ice trap, both condensing water, methanol, ammoniated water, and other products if any. Every sampling corresponds to the accumulated condensation since the previous sampling, and sampling rate is about twice per hour. The samples taken were then analyzed by GC–FID (Perkin–Elmer Clarus 500), with on-column injection onto a 5 m pre-column connected to a 30 m (DB-WAX 30 m × 0.53 mm × 50 μm) capillary column. The temperature program started at 100 °C and increased until 210 °C with a 10 °C min^{-1} rate and then stayed 5 min at 210 °C, while helium was flushed with a 12 psig inlet pressure. GC–MS analysis was also performed on a 30-m (ELITE-WAX ETR 30 m × 0.25 mm × 0.5 μm) capillary column. The temperature program starts at 70 °C and increases until 240 °C with a 10 °C min^{-1} rate, then stays 10 min at 240 °C, while helium is flushed at a 2 $ml\ min^{-1}$ flow rate.

3. Results and discussion

3.1. Ammoniation: an acid–base reaction

Converting esters into nitriles consists of a series of acid–base reactions, and both academic and patent literature focused their attention on searching catalysts with acid–base features. High redox features are also more susceptible of enhancing side-reactions, thus reported catalysts are mostly supported metal oxides actually. Catalysts with amphoteric character such as zinc, gallium, indium, zirconium, or aluminum oxides gave better results than catalysts such as the basic MgO or the acidic V_2O_5 or WO_3 in the present process. Besides, it was also pointed out that too strong acid sites were the source of side-reactions toward polymers or resins [22]. Early steps of the transformation include the production of methanol, which can be transformed into formaldehyde, which can be performed by transition metal oxide catalysts such as titania or supported vanadia [23], and foul the catalyst or produce methylamine [6] which is a problem for effluent treatment. Methanol can also be activated by the catalyst and induce methylation of amides; thus, redox features have to be carefully observed. Although acid–base features seem to be the key to efficient nitrilation of acids or esters, no correlation between measured amounts or nature of these sites and any step of this transformation was already investigated, to our knowledge, most probably because the several steps do not necessarily get catalyzed by the same features. Adsorption microcalorimetry appears as a perfectly dedicated technique to investigate these acid–base features, and the purpose of this article is to observe which nature and strength of acidic, basic, or both features can correlate with the rate-determining step of the present reaction, whatever the elements composing the catalyst. Acid–base features of tested catalysts are presented in Table 1.

3.2. Stability toward harsh conditions

Experimental conditions are especially harsh and thus catalysts have to sustain high temperature and high partial pressure of ammonia, water, and methanol. For example, oxides of zinc and to a lesser extent of indium were observed to be leached by carboxylates and ammonia [3,24], vanadium oxide can also be leached by water and acids, and titania was observed to be leached in the present conditions (pink color appearing in the condensate). Heteropoly acids are also quite unstable under high pressure of ammonia, for ammonium cations can proceed to exchanges inside their structure [25]. In the case of cesium heteropoly tungstate, cesium cations may be replaced by ammonium and therefore change the acid–base properties and lead to leaching of cesium salts out of the catalytic bed. Boron-containing aluminas are also good acidic catalysts that are however also sensitive to water partial pressures [20]. Microcalorimetric study and chemical analysis of used 5%B/Al_2O_3 catalyst was performed and it could be observed that no boron was leached out of the catalyst's surface but that some coking took place (about 0.5 wt% of carbon) and that the overall acidity was reduced by about 10% of all strengths, most probably due to covering of sites by coke.

Besides, the size of the fatty compounds can hinder their access to a part of the active sites; this problem can be encountered with some micro- and mesoporous catalysts. The presence of micropores could generate selective adsorption of methanol, ammonia or water in places inaccessible to fatty molecules and could act as a source of methylation of amides or other side-reactions, by

Table 1
Surface properties, ester conversion, and nitrile yield for catalysts tested for 4.4 s contact time at 300 °C.

Label	Catalyst	Surface[a] (m^2/g)	Pore size[b] (nm)	Volume (ml)	Mass (g)	Acidic sites[c]		Basic sites[c]	Results at 300 °C			Literature
						N ac. sites (μmol/g)	N strong ac. sites (μmol/g)	N bas. sites (μmol/g)	Conversion (mol%)	Nitrile yield (mol%)	NMA[4] (mol%)	Nit. yield (mol%)
X	Glass beads (blank)	–		1.5	–	0.0	0.0	0.0	0	0	0.0	
Acidic solids												
A	24%WO_x/ZrO_2	112.05		1.5	1.0892	190.5	142.0	11.2	98	96	1.0	
B	Nb_2O_5	106.5	5.6	1.5	1.2322	170.4	64.3	10.7	98	97	1.1	98.1[A]
C	Phosphated ZrO_2	130.3		1.5	1.5997	254.1	90.9	27.0	98	95	2.1	
D	3%B/Al_2O_3	266	9.0	1.4	0.9455	345.8	123.2	–	82	77	3.8	
E	5%B/Al_2O_3	239	8.1	1.45	1.0088	454.1	177.0	40.0	71	66	2.6	
F	Faujasite HY Si/Al 5.1	730	0.5	1.5	0.7220	450.0	100.0	–	70	53	7.7	
G	Bentonite	186.6	6.0	1.5	0.8680	380.0	60.0	–	64	54	5.8	
H	HPA/TiO2	33.3		1.5	1.5572	96.6	33.0	–	63	61	0.8	
I	H-MFI Si/Al 28	–		1.5	0.9117	–	–	–	44	34	3.7	
J	$NbOPO_4$	44.5		1.55	0.7240	106.8	38.9	6.5	43	42	0.8	
K	Phosphated SiO_2	91.4		1.5	1.2684	–	–	–	28	26	1.1	
L	$Cs_{2.5}H_{1.5}SiW_{12}O_{40}$	–		1.1	1.9540	–	–	–	13	8	1.5	
M	WO_3	3.5		1.5	2.3000	12.8	–	–	8	7	0.0	58.7[A]
N	$Cs_{3.0}PW_{12}O_{40}$	–		1.45	1.6675	–	–	–	7	5	0.2	
O	AlF_3 55%	50		1.5	0.9090	175.0	5.0	–	5	1	0.1	
P	B_2O_3	–		1.6	1.4272	–	–	–	0	0	0.0	
Amphoteric solids												
a	Al/ZrO_2	52.6		1.5	1.0981	94.7	55.7	191.5	98	96	0.6	
b	Zn/ZrO_2	57.5		1.5	1.0574	103.5	64.9	205.3	98	96	0.2	
c	16%WO_x/ZrO_2	88		1.5	1.2378	234.0	122.0	147.0	98	97	0.6	
d	TiO_2	50	11.6	1.5	0.1480	282.0	120.0	56.4	98	96	0.8	98.5[A]
e	Siralox 30	496	7.1	1.5	0.7410	297.6	147.2	90.0	98	96	2.6	
f	7%WO_x/ZrO_2	87.3	6.9	1.5	1.5680	192.1	74.9	140.0	97	94	0.7	
g	γ-Al_2O_3 (BASF)	196		1.5	0.8655	170.2	69.9	–	96	93	0.6	96.5[B]
h	Fe/ZrO_2	73.6		1.5	0.9675	110.4	74.3	220.8	96	90	0.4	96.2[C]
i	ZrO_2	53		1.5	1.8129	80.0	45.0	196.1	95	95	0.1	98.2[A] 96.7[C]
j	Fe_2O_3	141		1.5	1.8386	140	30	400	95	94	0.6	98.1[A]
k	Co/ZrO_2	68.3		1.5	1.0891	61.5	29.1	107.2	93	91	0.3	
l	Siralox 40-450	600	6.9	1.5	0.5534	282.0	149.1	90.0	89	83	3.1	
m	γ-Al_2O_3 [18]	420		0.85	0.5930	350	60	540	73	59	1.0	96.5[B] 98.9[A]
n	ZnInOx (3:1)	41		1	0.7500	68.1	49.3	176.3	62	62	0.3	
o	ZnInOx (19:1)	37		1.5	0.8320	81.0	43.7	155.4	42	40	0.0	
p	ZnInOx (9:1)	57		1.1	0.3500	98.0	56.4	241.1	39	37	0.2	
q	γ-Al_2O_3 (DEGUSSA)	115	9.6	1.5	0.1300	197.8	84.3	165.6	24	9	2.5	96.5[B] 98.9[A]
r	ZnO	5		1.5	1.1188	20.5	8.6	22.3	12	12	0.2	98.5[A]
Basic solids												
α	Hydroxyapatite	99.8		1.5	0.6550	121.8	*0.0*	210.0	37	28	1.2	
β	Hydroxyapatite 1.66	137.4		1.55	0.7770	144.3	9.3	320.0	30	10	2.0	
γ	Hydrotalcite Mg/Al = 3	120		1.5	1.7215	57.2	0.0	587.0	5	0	2.5	
δ	MgO	50		1.5	1.0700	1.0	0.0	200.0	4	2	0.0	
ε	Hydrotalcite	80		1.5	1.0639	18.4	0.0	265.6	3	2	0.2	

[a] BET surface area.
[b] Mean pore size as calculated by the BJH method on mesopores as 4 V/A.
[c] Measured by adsorption calorimetry of NH_3 (acid-) and SO_2 (basic sites).
[A] Patent JP 04-208260 (about 4–13 s mean residence time).
[B] Patent JP 04-283549 (13 s).
[C] Patent JP 10-195035 (5 s).

creating spots with high concentration of these molecules. Condensation of fatty molecules inside the pores could also enhance side-reactions, since in liquid phase, distances between molecules are importantly decreased and since concentrations of heavier molecules are considerably higher than in the gas phase. Using the Barrett–Joyner–Hallenda method (with nitrogen at −195.8 °C) on several mesoporous catalysts presented in Table 1, the smallest measured mean pore size is 5 nm. It can be evaluated from the Kelvin equation that the partial pressure at which pore condensation occurs in a 5 nm pore at 300 °C is about 0.4 bar for lauramide (which stands as the most susceptible of condensing among main molecules). Since the maximum reachable pressure for fatty compounds is capped at 0.13 bar, this is the feed concentration, no pore condensation should occur inside mesopores at 300 °C.

3.3. Diffusion limitations on silica–alumina and niobium oxide

In order to compare catalysts with each other, the mean residence time was kept similar and physical limitations have been

avoided. Diffusion limitations were evaluated at temperatures lower than 300 °C for the purpose of posterior investigations: at 250 °C on a Siralox 30 silica–alumina and at 200 °C on niobium oxide. In the range of gas velocity and particle size where no diffusion limitation occurs at 200 and 250 °C, there should also be no limitations at higher temperature, that is, 300 °C here. Both catalyst/temperature couples were chosen for their intermediate conversion ranges (that is, 20–60 mol%) for a 4.4-s contact time, since the variations are easier to evaluate. On Siralox 30, external diffusion limitations were not detected below at least 7.5 mm s^{-1} linear velocity, whereas internal diffusion limitations could be observed for particle size higher than about 200 μm. On niobium oxide, external diffusion limitations could be observed above 6.8 mm s^{-1} linear velocity, and internal diffusion limitation also for particle size higher than about 150 μm. Patent literature does not disclose particle size parameters; however by the choice of linear velocity (see Table 2), it is implicitly stated that no external diffusion limitation occurs until 22.4 mm s^{-1}.

3.4. Correlations between acid–base properties and conversions

Several catalysts were proposed for this reaction in patents, and Table 2 reports the experimental conditions described by recent patent literature concerning conversion of lauric acid or methyl laurate. Several different conditions were used, but the ammonia to ester ratio was always at a value of about 4. Results reported by Akikubo and Takoaka in 1992 [9] correspond to contact times that can be evaluated at about 4–13 s, which is in the same order of magnitude as the results presented in this article. Apart from zinc oxide, some aluminas and tungsten oxide, these results are in agreement with the ones presented here (see Table 1). However, their experimental conditions concerning the high volume catalytic bed (11 l) are significantly different: it is filled at about 0.5% of the total volume, thus in the form of a very thin disc, and with a significantly slower gas linear velocity of 0.3 mm s^{-1} (present article: 6.8 mm s^{-1}). Results from 1998 [10] correspond to contact time and gas velocity similar to the present experiments and zirconia-based catalysts perform here as well as in this patent.

Table 1 reports the ester conversion, the nitrile and N-methyl amide yields, as well as the acid–base features measured by adsorption microcalorimetry. Glass beads of 1 mm diameter were used as a reference in order to evaluate the reaction without catalysis in same conditions, and it can be observed that no ester is converted at 300 °C without catalyst for a 4.4-s contact time. Then, for gas-phase ester conversion into nitrile, the catalyst has to play on both aminolysis and dehydration, contrary to what is usually asked from catalysts in liquid phase for which the first step can occur without catalyst [3,26]. It can be globally observed in Table 1 that basic catalysts are quite inefficient, while acidic and amphoteric catalysts perform mostly well.

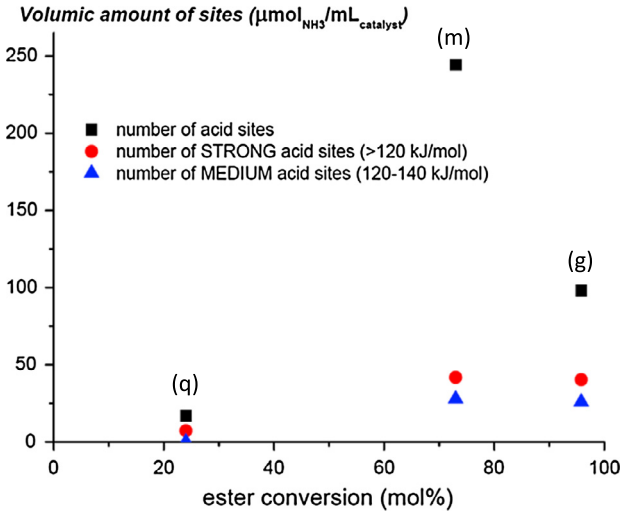

Fig. 2. Volumic amounts of acid sites, strong and medium strength acid sites as a function of the methyl laurate conversion for the three aluminas labeled g, m, and q in Table 1.

Different results can be obtained for a same nature of catalyst: the three γ-alumina catalysts display significantly different efficiencies in this test. The volumic amounts of acid, strong, and medium strength acid sites are plotted in Fig. 2 for three aluminas (labels g, m, and q in Table 1) as a function of their ester conversion. The alumina (m) with the highest BET surface area does not display the best conversion, nor is it the total volumic density of acid sites that determines the best efficiency among these aluminas, but more probably the amount of high or medium strength acid sites.

Considering the whole list of catalysts, the volumic amount of strong acid sites (adsorption strength of ammonia higher than 120 kJ mol^{-1}) was found to display good correlation with both ester conversion and nitrile yield, as can be observed in Fig. 3. A quasi-linear dependency of conversion and nitrile yield appears for the volumic amount of strong acid sites below 50 μmol $ml^{-1}_{catalyst}$, and then, maximum conversion is reached for the present conditions of 300 °C working temperature and ester flow rate of 2 μmol s^{-1} (this is 1.5 g h^{-1}). Once made sure that no diffusion limitations occur, if these sites are responsible of the rate-determining step, then

Table 2
Parameters of the recent patent literature.

Patent	JP 04-208260	JP 04-208260	JP 04-283549	JP 10-195035	This article
Publication year	1992	1992	1992	1998	
Temperature	300 °C	300 °C	300 °C	300 °C	300 °C
Mass cata. (g)	1	138		1	0.1–2
Reactant (lauric)	Ester	Ester	Acid	Ester	Ester
Tested catalysts	Metal oxides	Metal oxides	Alkali treated γ-Al_2O_3	Impregnated ZrO_2	Metal oxides
Vol. reactor (ml)	23.6	11309.4	124.7	2.4	1.6
Cross section (cm^2)	0.785	314.150	3.464	0.785	0.503
Actual catalyst volume (ml)	1–2	30–60	100	0.80	1.50
Flow rates (ml/h) NH_3	438	22,400	22,200	500	600
(g/h) ester	1	50	50	1	1.51
Flow rates (mol/h) NH_3	0.0188	0.9619	0.9533	0.0215	0.0258
(mol/h) ester	0.0047	0.2333	0.2333	0.0047	0.0070
Ratio NH_3/ester	4.0	4.1	4.1	4.6	3.7
MRT full bed (s)	153.2	1204.0	16.0	13.8	4.7
Actual MRT (s)	6.6–13.2	3.8–7.7	12.9	4.7	4.4
Linear velocity (mm s^{-1})	1.96	0.30	22.44	2.18	6.77

the turnover frequency corresponding to these conditions can be evaluated at about 3×10^{-2} s^{-1}.

Similarly, good correlation is observed in Fig. 4 with the volumic amount of medium strength acid sites (ammonia adsorption's strength between 120 and 140 kJ mol^{-1}). This fits better with boron-containing aluminas (high amount of strong acidity and average nitrile yield) and literature indicates how too strong acidity can be the source of side-reactions (such as coking) that can foul the active surface and block the access to reactants. Thus, a population of too strong acid sites could be discarded, by deciding a maximum strength (measured by NH_3 adsorption calorimetry) above which sites are fouled or useless to the catalysis.

Catalytic test results do not lead to any correlation with basic sites, and correlation with the total number of acid sites raises several exceptions, such as hydroxyapatite, aluminum fluoride and hydrotalcite, which display high amount of acid sites but bad conversion nitrile yield; besides, faujasite Y ratio 5.1, bentonite, and a γ-alumina perform only slightly above 50 mol%, while displaying very high amounts of acid sites. This is the reason why a better correlation was sought with only a fraction of the total number of acid sites.

3.5. N-methyl amide formation

In Fig. 5 are plotted the yields of N-methyl amide as a function of the mean pore diameter calculated by the BJH method on the silica–aluminas, a bentonite, niobium oxide, boron-containing aluminas, alumina (DEGUSSA), the HY faujasite, the 7% tungstated zirconia, and titania. Results on faujasite and ZSM-5 discard any problem of spatial constraint, and then, the globally decreasing yield with increasing pore size could stem from some degree of condensation inside the pores. Kelvin equation was used to evaluate the lauramide saturation pressure for small pore size at 300 °C (Fig. 5), and it appears that condensation could only take place in pores smaller than 1.7 nm in the present case (ester partial pressure of 0.125 bar). Then, condensation should only happen in micropores and N-methylation might be enhanced in condensed medium. A second hypothesis concerning the origin of N-methyl amide is the reaction of amide with ester. In both scenarios, amide accumulation necessarily improves N-methylation; however, there is no direct monitoring of amide inside the catalytic bed, and then, the amount of amide analyzed at the end of the bed is probably underestimating its accumulation. No clear correlation of N-meth-

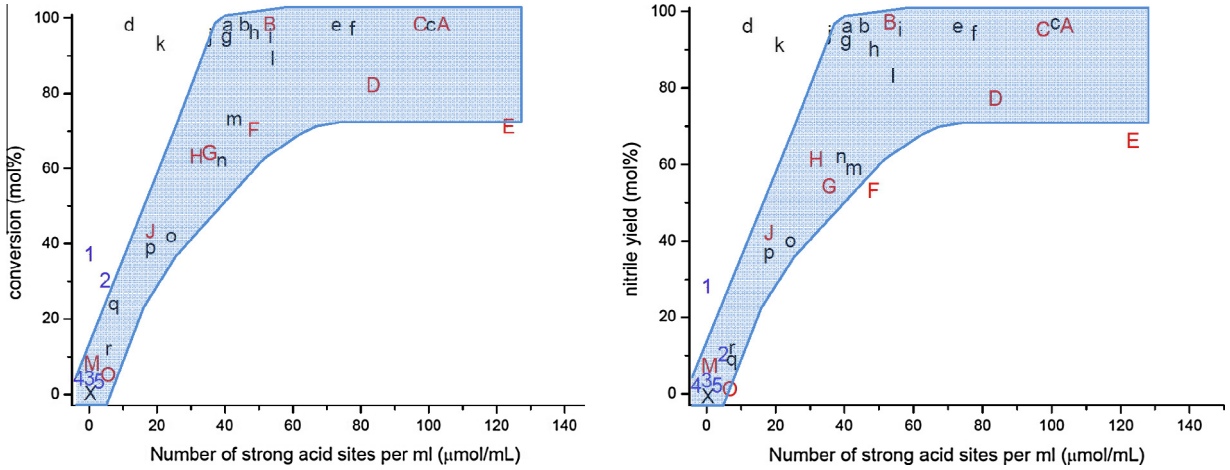

Fig. 3. Conversion of ester and nitrile yield (mol%) as a function of the volumic density of strong acid sites (μmol ml^{-1}). Labels are reported in Table 1 and colors are referring to acidic (red), basic (blue), and amphoteric (black) solids. (For interpretation of the references to color in this figure legend, the reader is referred to the web version of this article.)

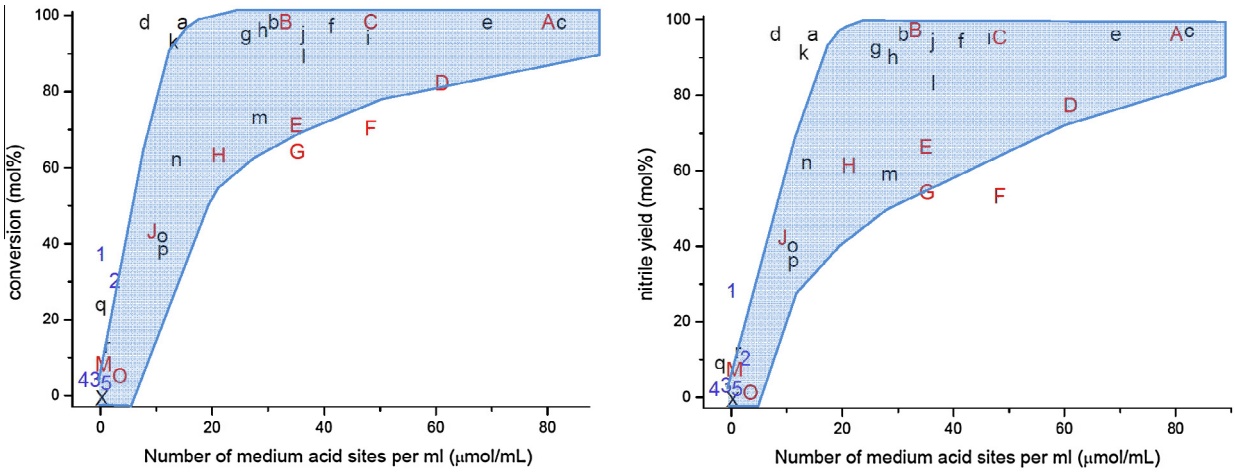

Fig. 4. Conversion of ester and nitrile yield (mol%) as a function of the volumic density of medium acid sites (μmol ml^{-1}). Labels are reported in Table 1 and colors are referring to acidic (red), basic (blue), and amphoteric (black) solids. (For interpretation of the references to color in this figure legend, the reader is referred to the web version of this article.)

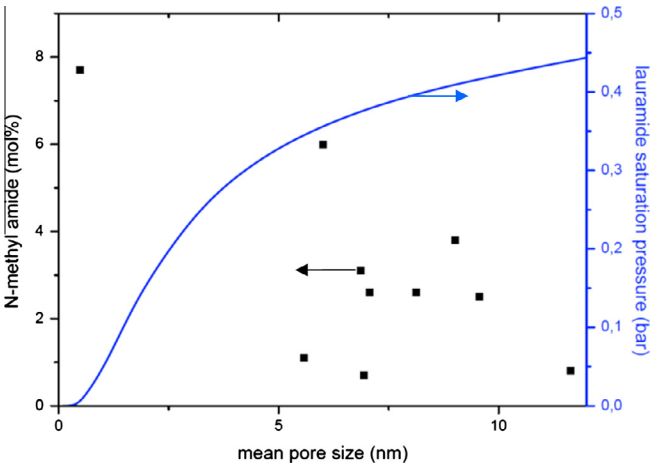

Fig. 5. N-methyl lauramide yield as a function of the mean pore size calculated by the BJH method (black squares) and the lauramide saturation pressure in the pores, as calculated by the Kelvin equation (curve).

ylation could be observed with lauramide or with lauric acid content, which would be a product of amide N-methylation by the ester, was only detected in very small amounts by GC–FID and GC–MS.

The amounts of N-methyl-lauramide at 300 °C are reported in Table 1. The HY faujasite, H-MFI, bentonite, high surface silica alumina, hydrotalcite, one alumina (DEGUSSA), and boron-containing aluminas are the catalysts displaying the highest yields of N-methyl amide. Impregnated zirconias, niobium oxide and phosphate, heteropolyacids, and hydroxyapatites also display about 1 mol% of it. Some global tendency can be observed between the introduced surface of catalyst (BET surface area multiplied by the introduced mass) and the yield of N-methyl amide, which lets us assume that the N-methylation happens on the surface. Methylation of amides needs an "activated" form of methyl (usually methyl halogenide), which can be here a methoxy adsorbed on the catalyst. Alkali-exchanged Y faujasites (pore size about 0.75 nm) and ZSM-5 (pore size about 0.55 nm) were tested by Fu and Ono [27] for the N-methylation of aniline with dimethyl carbonate, and it was observed that spatial constraints (not the case here) and both base features and weakly acidic sites were crucially enhancing the efficiency of this reaction. Both HY faujasite and ZSM-5 (H-MFI) tested here display almost no mesoporosity but high microporosity. On the present list of catalysts, no clear correlation appeared with any acid–base features.

3.6. Rate-determining step: Brønsted or Lewis acid catalysis

About the nature of the rate-determining step, it can be observed that at 300 °C, on most catalysts the amide accumulation is rather low, which gives credit to assuming that the conversion of ester into amide is the slowest part, rather than the dehydration of amide. Moreover, the dehydration reaction can only happen after the ester conversion into amide, which implies a shorter time of contact of amide with the catalyst, and though at 300 °C it does not lead to much accumulation. Aminolysis of ester can consist in one concerted mechanism or in two steps through a hemiaminal intermediate. A DFT study of the conversion of methyl ester into amide catalyzed by a base suggested that the two-step scenario was the most energetically favorable, and the first step of nucleophilic attack by ammonia appears as the rate-limiting step. The addition of a molecule of ammonia or methanol to this system was also calculated to reduce the energy barriers on both steps [28]. Amidation of esters assisted by salts ($Mg(OCH_3)_2$, $CaCl_2$, $NaOCH_3$) in stoichiometric amount was also investigated in methanol at 80 °C and the metal cation is thought to assist in the nucleophilic attack of ammonia, possibly like a Lewis acid, while imide is proposed as an intermediate [29]. This imide, or N,N-diamide, could be the product of reactions between two amide molecules and could react on the catalyst surface into a nitrile and a by-product; however, no scenario related to this hypothesis could be supported by the present tests. Both Lewis and Brønsted acid features exist on the tested catalysts, but some are mainly Lewis (most impregnated zirconias do not display any infrared signature of Brønsted acidity) while other possess more Brønsted sites (niobium oxide [30], α-Fe_2O_3, tungstated zirconias [19]). Concerning the conditions of the present catalytic test and the relevancy of Lewis or Brønsted sites, it can be pointed out that at 300 °C, under flow of ammonia and produced stream of water in stoichiometric amount, the catalyst surface's medium and strong sites should be covered by ammonia or water derived molecules, and then only the weak sites, that is, most probably not the Lewis sites, would be accessible. However, in case of niobium oxide, it was observed that Lewis acid sites were still accessible and catalytically active when immerged in water at 120 °C [31,32], which are conditions less favorable to the stability of Lewis sites than in the present article; thus, if we can generalize to other presently studied catalysts, it can be assumed that some or all of these sites are still catalytically active here.

If Lewis sites are still active to promote the nucleophilic attack of ammonia by pulling on the methoxy, we still need to know the whereabouts of ammonia. Guimon et al. discussed how at high temperatures ammonia could dissociatively adsorb onto metal oxide surface and interact with Lewis acid sites and surface oxygens to convert them into adsorbed $-NH_2$ and a Brønsted acid site [33]. This appears however conflictual with earlier statements about the necessity of Lewis sites. Moreover, there is no certainty about whether ammonia is attacking the nucleophilic carbon of the ester function as an ammonium (adsorbed on a Brønsted site) or as $-NH_2$ (adsorbed dissociatively on a Lewis site) or even as a physisorbed NH_3 molecule.

Variation of ammonia partial pressure from 0.25 to 0.625 bar on zinc oxide (label "r," almost no amide accumulation) and hydroxyapatite (label "β," high amide accumulation) at 300 °C, keeping everything else constant (ester flow rate, total flow rate, overpressure), was observed to keep the ester conversion and nitrile yield almost unchanged. The global reaction order for the ammonia partial pressure is evaluated for zinc oxide at about 0.15 or below, and for hydroxyapatite at about 0.10 or below. This could mean that in the standard conditions (0.5 bar partial pressure), ammonia is not limiting either ester conversion or amide dehydration. As a consequence, the reactive form of ammonia is probably an adsorbed form at the surface of the catalyst, and the equilibrium between gas-phase ammonia and this reactive form is not limiting the kinetics.

3.7. Dehydration of amides

In the scenario where ester aminolysis is the rate-determining step, correlation with the nitrile yield brings no information on which feature influences amide dehydration. Studies in liquid (diluted) phase can be found in the literature. Enthaler et al. have been reporting zinc and iron homogeneous catalyzed dehydration of amides in toluene, providing 3.5 stoichiometric amounts of silylation, where zinc (or iron) acts as a Lewis acid helping with the silylation on the nitrogen atom [34]. A study by Furuya et al. on dehydration of amides using perrhenic acid ($ReO_3(OH)$) at 1 mol% in toluene or mesitylene proposes a pathway via a six-membered cyclic transition state [35,36], thus also with a Lewis acid site. In the present case, there is no evidence that the dehydration does not occur out of the catalyst surface or proximity; however, it

should be energetically more favorable to perform it in the vicinity of Lewis acid sites or of labile protons, that is, ammonium cations here. Besides, this dehydration is known to proceed slowly without catalyst [3]. Experiments starting from the amide could not be carried out, since the present process requires a liquid reactant (peristaltic pump control) and lauramide is only slightly soluble (less than 1 mol%) in methanol or methyl laurate, and no other inert solvent could be found to provide high partial pressure of amide while bringing no additional side-reaction at the surface of the catalyst.

4. Conclusion

Several catalysts were tested for the ammoniation–dehydration of lauric acid methyl ester into nitrile in a gas-phase continuous downstream process, at 300 °C, with an ester flow rate of 1.5 g h^{-1} and a mean residence time of 4.4 s. Catalysts tested in the patent literature were discussed and compared to the present results. A reference experiment carried out with glass beads showed that no ester was converted in the present conditions without a catalyst. It was observed that the rate-determining step in this reaction, that is, ester conversion, was controlled by the volumic density of medium strength acid sites (ammonia adsorption energy between 120 and 140 kJ mol^{-1}) and was most probably assignable to the attack of the nucleophilic carbon by an adsorbed form of ammonia. This would correspond to a turn-over frequency of about 3×10^{-2}. No correlation with basicity was observed, and furthermore, basic catalysts displayed poor efficiency. The dehydration of amide occurs at the surface of the catalysts and is helped by the presence of labile protons in the form of ammonium. The formation of N-methyl lauramide as a side-product occurs mainly for high surface catalysts with a porous system with mean pore size lower than 10 nm. It is related with amide accumulation and could be due to reaction between amide and ester.

Acknowledgments

The authors are thankful to the scientific services of IRCELYON. The research leading to these results has received funding from the European Union Seventh Framework Programme (FP7/2007–2013) under grant agreement no. 241718 EuroBioRef.

References

[1] J.L. Dubois, Patent WO 2010103223, to Arkema, 2010.
[2] N.M. Irving, Canadian Patent 2687816, to Rio Oeste S.A., 2008
[3] A. Mekki-Berrada, S. Bennici, J.P. Gillet, J.L. Couturier, J.L. Dubois, A. Auroux, Ammoniation-dehydration of fatty acids into nitriles: heterogeneous or homogeneous catalysis?, ChemSusChem, http://dx.doi.org/10.1002/cssc.201300210.
[4] G.D. Van Epps, E.E. Reid, J. Am. Chem. Soc. 38 (1916) 2128.
[5] A. Mailhe, Bull. Soc. Chim. 4 (23) (1918) 232.
[6] J.A. Mitchell, E.E. Reid, J. Am. Chem. Soc. 53 (1931) 321–330.
[7] A.W. Ralston, US Patent 1991955, to Armour and Company, 1935; A.W. Ralston, W.O. Pool, J. Harwood, US Patent 2033537, to Armour and Company, 1936.
[8] C.G. Wortz, US Patent 2205076, to du Pont de Nemours, 1940.
[9] A. Akikubo, H. Takaoka, Japanese Patent 04-208260, to Lion corp., 1992; A. Akikubo, H. Takaoka, A. Sato, Japanese Patent 04-283549, to Lion corp., 1992.
[10] H. Takaoka, T. Okada, T. Inagaki, Japanese Patent 10-195035, to Lion corp., 1998.
[11] M. Qi, D. Wang, J. Li, Y. Konh, B. Wang, Q. Dong, Chinese Patent 101579639 (A), to Jiangsu Youth Chemical Co Ltd., 2009
[12] F.B. Bizhanov, E.Kh. Yazbaev, Zh. Prnazarov, Izv. Akad. Nauk. Kazakh. SSR, Ser. Khim. 4 (1985) 23–26.
[13] C. Gennequin, T. Barakat, H.L. Tidahy, R. Cousin, J.-F. Lamonier, A. Aboukaïs, S. Siffert, Catal. Today 157 (2010) 191–197.
[14] D. Stosic, S. Bennici, S. Sirotin, C. Calais, J.-L. Couturier, J.-L. Dubois, A. Travert, A. Auroux, Appl. Catal. A: Gen. 447–448 (2012) 124–134.
[15] C. Lamonier, J.-F. Lamonier, B. Aellach, A. Ezzamarty, J. Leglise, Catal. Today 164 (2011) 124–130.
[16] F. Lefebvre, F.X. Liu-Cai, A. Auroux, J. Mater. Chem. 4 (1994) 125–131.
[17] A. Loustaunau, R. Fayolle-Romelaer, S. Celerier, S. Brunet, J. Fluorine Chem. 132 (12) (2011) 1262–1265.
[18] A. Mekki-Berrada, D. Grondin, S. Bennici, A. Auroux, Phys. Chem. Chem. Phys. 14 (2012) 4155–4161.
[19] R. Kourieh, S. Bennici, A. Auroux, J. Therm. Anal. Calorim. 99 (2010) 849–853; R. Kourieh, S. Bennici, M. Marzo, A. Gervasini, A. Auroux, Catal. Commun. 19 (2012) 119–126.
[20] J.-L. Dubois, S. Fujieda, Stud. Surf. Sci. Catal. 91 (1995) 833–842.
[21] A. Mekki-Berrada, A. Auroux, in: M. Che, J. Vedrine (Eds.), Characterization of Solid Materials and Heterogeneous Catalysts: From Structure to Surface Reactivity, Thermal, Methods, vol. 2, Wiley-VCH Verlag GmbH & Co. KGaA, Weinheim, Germany, 2012, pp. 747–872 (Chapter 18), http://dx.doi.org/10.1002/9783527645329.ch18.
[22] M. Guisnet, P. Magnoux, Catal. Today 36 (4) (1997) 477–483.
[23] J. Döbler, M. Pritzsche, J. Sauer, J. Am. Chem. Soc. 127 (31) (2005) 10861–10868.
[24] W. Zhao, W. Peng, D. Wang, N. Zhao, J. Li, F. Xiao, W. Wei, Y. Sun, Catal. Commun. 10 (5) (2009) 655–658.
[25] J.S. Santos, J.A. Dias, S.C.L. Dias, F.A.C. Garcia, J.L. Macedo, F.S.G. Sousa, L.S. Almeida, Appl. Catal. A: Gen. 394 (2011) 138–148.
[26] E.T. Roe, J.M. Stutzman, J.T. Scanlan, D. Swern, J. Am. Oil Chem. Soc. (1952) 18–22.
[27] Z.H. Fu, Y. Ono, Catal. Lett. 18 (1993) 59–63.
[28] J. Mielby, A. Riisager, P. Fristrup, S. Kegnaes, Catal. Today 203 (2013) 211–216.
[29] M.W. Bundesmann, S.B. Coffey, S.W. Wright, Tetrahedron Lett. 51 (2010) 3879–3882.
[30] D. Stosic, S. Bennici, V. Rakic, A. Auroux, Catal. Today 192 (2012) 160–168.
[31] K. Nakajima, Y. Baba, R. Noma, M. Kitano, J.N. Kondo, S. Hayashi, M. Hara, J. Am. Chem. Soc. 133 (2011) 4224–4227.
[32] A. Corma, F.X. Llabres i Xamena, C. Prestipino, M. Renz, S. Valencia, J. Phys. Chem. C 119 (2009) 11306–11315.
[33] C. Guimon, A. Zouiten, A. Boreave, G. Pfister-Guillouzo, P. Schultz, F. Fitoussi, C. Quet, J. Chem. Soc. Faraday Trans. 90 (22) (1994) 3461–3467.
[34] S. Enthaler, S. Inoue, Chem. Asian J. 7 (2012) 169–175; S. Enthaler, J. Org. Chem. (2011) 4760–4763; S. Enthaler, M. Weidauer, Catal. Lett. 141 (2011) 1079–1085.
[35] S. Sueoka, T. Mitsudome, T. Mizugaki, K. Jitsukawa, K. Kaneda, Chem. Commun. 46 (2010) 8243–8245.
[36] Y. Furuya, K. Ishihara, H. Yamamoto, Bull. Chem. Soc. Jpn. 80 (2007) 400.